Manuscript #MOLN-D-14-00306 (Revised)

Mol Neurobiol. 2014 Nov 7. [Epub ahead of print]
PMID: 25377796

DOI
10.1007/s12035-014-8965-5

Progranulin deficiency reduces CDK4/6/pRb activation and survival of human neuroblastoma SH-SY5Y cells

Ana de la Encarnación[1], Carolina Alquézar[1,2], Noemí Esteras[1,3] and Ángeles Martín-Requero[1,2]

[1]Department of Cellular and Molecular Medicine, Centro de Investigaciones Biológicas (CSIC) Madrid, [2]CIBER de Enfermedades Raras (CIBERER). [3] Present address: Department of Molecular Neuroscience, Institute of Neurology, London.

Key words: Progranulin FTLD-TDP, CDK6/pRb, PI3K/Akt, ERK1/2, cell survival, apoptosis

Address for correspondence:

Dr. Ángeles Martín-Requero

Centro de Investigaciones Biológicas (CSIC)

Ramiro de Maeztu 9

28040 Madrid, SPAIN

Phone: 34-91-837-3112

Fax: 34-91-536-0432

Email: amrequero@cib.csic.es

ABSTRACT

Null mutations in *GRN* are associated with Frontotemporal Lobar with TDP-43 inclusions (FTLD-TDP). However the influence of progranulin (PGRN) deficiency in neurodegeneration is largely unknown. In neuroblastoma cells, silencing of *GRN* gene causes significantly reduced cell survival after serum withdrawal. The following observations suggest that alterations of the CDK4/6/pRb pathway, secondary to changes in PI3K/Akt and ERK1/2 activation induced by PGRN deficiency, are involved in the control of serum deprivation-induced apoptosis. (i) Inhibiting CDK4/6 levels or their associated kinase activity by sodium butyrate or PD332991 sensitized control SH-SY5Y cells to serum deprivation-induced apoptosis without affecting survival of PGRN deficient cells. (ii) CDK4/6/pRb seems to be downstream of the PI3K/Akt and ERK1/2 signaling pathways since their specific inhibitors, LY294002 and PD98059, were able to decrease CDK6-associated kinase activity and induced death of control SH-SY5Y cells. (iii) PGRN deficient cells show reduced stimulation of PI3K/Akt, ERK1/2 and CDK4/6 activities compared with control cells in the absence of serum. (iv) supplementation of recombinant human PGRN was able to rescue survival of PGRN deficient cells. These observations highlight the important role of PGRN-mediated stimulation of the PI3K/Akt-ERK1/2/CDK4/6/pRb pathway in determining the cell fate survival/death under serum deprivation.

INTRODUCTION

The term Frontotemporal Lobar Degeneration (FTLD) refers to a group of progressive brain rare diseases, which involve shrinkage of specific areas of the brain that regulate behavior, personality and language. The onset of symptoms usually occurs before the age of 60 years, accounting for 5-10% of dementia patients [1,2].

The neuropathological hallmark of FTLD is the degeneration of frontal and temporal lobes, as well as the accumulation of protein inclusions in neuronal and glial cells [3]. FTLD subtypes have been established depending on the proteins found in these inclusions. The main subtypes are FTLD-tau and FTLD-TDP for microtubule associated protein tau (MAPT) and FTLD-TDP for ubiquitinated transactive response DNA-binding protein 43 (TDP-43) positive inclusions respectively [4-6]. A large subset of FTLD-TDP patients has been identified to harbor loss-of-function mutations (including null mutations) in the gene encoding progranulin (*GRN*) [7,8], and a smaller number of mutations in the *valosin-containing protein* (*VCP*) gene [9], *transactive response (TAR) DNA-binding protein-43* (*TARDBP*) [10] *sequestome1/p62* (*SQSTM1*) [11] and *ubiquilin-2* (*UBQLN2*) [12]. A *C9ORF72* hexanucleotide expansion in chromosome 9 has been described to be responsible for familial Frontotemporal Dementia overlapping with motor neuron disease (FTD-MND) cases and amyotrophic lateral sclerosis (ALS) [13,14]. *GRN* mutations are dominantly inherited and the disease mechanism is postulated to be haploinsufficiency, as most *GRN* mutations lead to an approximately 50% reduction in PGRN levels [15-17].

PGRN is a 593 amino acid, 86 kDa cysteine rich protein containing a signal peptide and 7.5 repeats of highly conserved granulin motifs [18]. PGRN is widely distributed [19], including the central nervous system (CNS) [20]. Previous research has suggested that PGRN may function as an autocrine neuronal growth factor involved in the inflammatory neuronal repair process in the CNS [21]. PGRN has been reported to promote neuronal survival in culture [22], though the degree of this effect is controversial [23]. The effects of PGRN deficit in the CNS have been also studied in *GRN* knockdown neuronal cells [24,25] and knockout mice (*GRN*-/-). The *GRN* silenced neuronal cells were shown to display some of the phenotypic characteristics of the disease such as increased cytosolic accumulation of TDP-43 and increased vulnerability of neurons to normally sublethal insults [25]. Increased caspase activation and decreased TDP-43 solubility was also found in *GRN* KD cortical neurons [26]. On the other hand, *GRN*-/- mice develop ubiquitin-positive aggregates and phosphorylated TDP-43, similar to FTLD-TDP patients

[27,28]. Thus, it seems that *GRN* KD neuronal cells is a suitable experimental model to study FTLD-TDP associated with loss-of-function *GRN* mutations.

Previous work from this laboratory highlighted the role of the CDK6/pRb pathway in controlling cell fate survival/death of peripheral cells from carriers of a loss-of-function *GRN* mutation, c.709-1G>A [29]. In this work, we have addressed the issue as to whether PGRN deficiency also modulates this cascade, and eventually cell survival in a neuroblastoma cell line. For this purpose, we used a stable clone of SH-SY5Y cells in which *GRN* expression was knocked down by a vector-based shRNA approach [24]. Compared with control cells, survival of *GRN* KD SH-SY5Y cells was severely reduced in serum-free medium. Our results suggest that alterations in the CDK4/6/pRb pathway, secondary to changes in the activity of the PI3K/Akt and ERK1/2 pathways induced by PGRN deficiency, are involved in the control of serum deprivation-induced apoptosis.

MATERIALS AND METHODS

Materials

All components for cell culture were obtained from Invitrogen (Barcelona, Spain). LY294002 and PD98059 were obtained from Calbiochem (Darmstadt, Germany). Progranulin (human recombinant) was obtained from Enzo (Zandhoven, Belgium). Elastase from human leukocytes, Epidermal growth factor (EGF), the 3-(4,5-dimethylthiazol-2-yl)-2,5 diphenyltetrazolium bromide reactive (MTT), and the inhibitor of histone deacetylases, sodium butyrate (SB), were obtained from Sigma-Aldrich (Tres Cantos, Spain). The inhibitor of CDK6/CDK4-associated kinase activity, PD332991, was obtained from Pfizer (Gronton, Connecticut, US). 4,6-diamino-2-phenylindole (DAPI) and insulin were obtained from Life Technologies (Eugene, Oregon, US). Antibodies used in this study are listed in Table 1. Poly (vinylidene) fluoride (PVDF) membranes were purchased from Merk Millipore (Billerica, Massachusetts, US). The enhanced chemiluminiscence (ECL) system was from Amersham (Uppsala, Sweden). Other reagents were of molecular biology grade.

GRN knockdown neuroblastoma SH-SY5Y cell lines

Stable *GRN* knockdown neuroblastoma SH-SY5Y cells (Clone # 207) was a generous gift from Drs. Joselin and Wu from the Center for Genetic Medicine (Northwestern University, Chicago, Il US). *GRN* knockdown was achieved by using pSUPERIOR RNAi construct as previously described [24]. The target sequence of 19 nucleotides targeted against nucleotides 207–226 (#207) of the human *GRN* mRNA was designed. The 64 nt short hairpin RNA sense and antisense primer sequences were 5'-gatccccggccactcctgcatctttattcaagagataaagatgcaggagtggccttttggaaa-3' and 5'agcttttccaaaaaggccactcctgcatctttatctcttgaataaagatgcaggagtggccgggg-3'.

The sense and antisense primer pairs were annealed and ligated into the pSUPERIOR vector (OligoEngine) according to manufacturer's instructions. The vector control was also stably introduced into SH-SY5Y cells to generate the control cell line.

MTT colorimetric survival assay

Active mitochondria of living cells can cleave MTT to produce formazan, the amount of which is directly proportional to the living cell number. Cell survival was assessed essentially as described [30]. Cells (60,000) were incubated with 0.25 μg/μl of MTT in a reaction volume of 200 μl. After the incubation,

DMSO was added to dissolve formazan crystals. Dye absorbance in viable cells was measured at 590 nm with 620 nm as a reference wavelength. Cell survival was estimated as the percentage of the value of untreated controls.

Assessment of apoptosis and caspases activity

Apoptosis was characterized by chromatin condensation/fragmentation, as determined by cell fixation followed by 4,6-diamidino-2-phenylindole (DAPI) staining and fluorescence microscopy examination.

The activation of executive caspases was investigated using the Vybrant® FAM Caspase-3 and 7 Kit (Invitrogen, Carlsbad, CA, USA) including FLICA reagent that is retained within the cell, if bound to the active caspase molecule. Control and *GRN* KD SH-SY5Y were resuspended in 300 µl of RPMI containing 10 µl of FLICA reagent and incubated in 5% CO_2 at 37ºC for 60 min. The cells were then washed and suspended in wash buffer provided by the kit. The samples were analyzed on the flow cytometer.

Immunoblotting analysis

Cells were harvested, washed in PBS and then lysed in ice-cold lysis buffer (50 mM Tris pH 7.4, 150 mM NaCl, 50 mM NaF, 1% Nonidet P-40), containing 1 mM sodium orthovanadate, 1 mM phenylmethylsulfonyl flouride (PMSF), 1 mM sodium pyrophosphate and protease inhibitor Complete Mini Mixture (Roche, Mannheim, Germany). 20 to 50 µg of protein from cell extracts were fractionated on a sodium dodecyl sulfate (SDS) polyacrylamide gel, and transferred to PVDF membrane. The membranes were then blocked with Bovine Serum Albumin (BSA) (Sigma) or dry milk and incubated with primary antibodies as is indicated in Table 1. The release of cytochrome c from the mitochondria was assessed after cell fractioning to get cytosolic and crude mitochondrial extracts as described [31], using the ApoTrack™ Cytochrome c Apoptosis Antibody Cocktail. Signals from the primary antibodies were amplified using species-specific antisera conjugated with horseradish peroxidase (Bio-Rad) and detected with a chemiluminiscent substrate detection system ECL (Amersham). The antibody specificity was checked by omitting the corresponding primary antibody in the incubation medium. Protein band densities were quantified using Image J software (National Institutes of Health, Bethesda, Maryland, USA) after scanning the images with a GS-800 densitometer from Bio-Rad and normalized by those of β-actin or α-tubulin. When indicated cytosolic or mitochondrial proteins were normalized by GAPDH and C-V-α or PDH-E1-α respectively.

Quantitative real-time PCR

Total RNA was extracted from cell cultures using Trizol® reagent (Invitrogen, Alcobendas, Madrid, Spain). RNA yields were quantified spectrophotometrically and RNA quality was checked by the A260/A280 ratio and on a 1.2% agarose gel to determine the integrity of 18S and 28S ribosomal RNA. RNA was then treated with DNase I Amplification Grade (Invitrogen, Alcobendas, Madrid, Spain). One microgram was reverse transcribed with the Superscript III Reverse Transcriptase kit (Invitrogen, Alcobendas, Madrid, Spain). Quantitative real-time polymerase chain reaction (PCR) was performed in triplicates using TaqMan® Universal PCR MasterMix No Amperase UNG (Applied Biosystems, Alcobendas, Madrid, Spain) reagent according to the manufacturer's protocol. Primers were designed using the Universal Probe Library for Human (Roche Applied Science, Madrid, Spain) and used at a final concentration of 20 μM. The sequences of the forward and reverse primers used are the following: for *GRN*, 5'-tctgtagtctgagcgctaccc-3' and 5'-agggtccacatggtctgc-3'; for β-actin, 5'-ccaaccgcgagaagatga-3' and 5'-ccagaggcgtacagggatag-3'. Real time quantitative PCR was performed in the Bio-Rad iQ5 system using a thermal profile of an initial 5-minute melting step at 95 ºC followed by 40 cycles at 95 ºC for 10 seconds and 60 ºC for 60 seconds. Relative messenger RNA (mRNA) levels of the genes of interest were normalized to β-actin expression using the simplified comparative threshold cycle delta-delta CT method ($2^{-[\Delta CT\ GRN\ -\Delta CT\ Actin]}$).

Statistical analysis

Statistical analyses were performed on GraphPad Prism 5 for Macintosh (La Jolla, CA, USA). All the statistical data are presented as mean ± standard error of the mean (SEM). Statistical significance was estimated by analysis of variance (ANOVA) followed by the Bonferroni`s test for multiple comparisons. Differences were considered significant at a level of $p<0.05$.

RESULTS

GRN knockdown increased the vulnerability of cells to serum deprivation

To study the effects of PGRN deficiency on cell survival, we took advantage of stable *GRN* knockdown SH-SY5Y (*GRN* KD cells), generated in Dr. Wu lab with a pSUPERIOR RNAi construct containing the target sequence corresponding to nucleotide sequences 207 to 226 specific for human *GRN* gene [24]. As shown in Fig. 1 A, B, a considerable decrease in *GRN* mRNA and protein content were observed in KD cells compared with control SH-SY5Y cells expressing the empty vector. After serum deprivation, we found marked differences in cell survival between control and *GRN* KD cells as assessed by the MTT assay. While in control cultures, a large number of cells still survive 4 days after serum deprivation, in PGRN deficient cells there was an important reduction in cell viability from the first day (Fig. 1C).

Extracellular PGRN protects *GRN* KD cells from serum deprivation-induced cell death

To explore whether PGRN is able to protect SH-SY5Y cells from serum withdrawal, we treated *GRN* KD cells with exogenous rhPGRN for 3 days. Fig. 2A shows that the addition of exogenous rhPGRN was able to increase the percentage of survival of PGRN deficient cells up to the levels found in control cells. The effect of rhPGRN disappeared when it was previously degraded by elastase (Fig. 2A). As shown in Fig. 2B, left panel, incubation of rhPGRN with 0.1 U/ml of elastase for three hours was sufficient to completely degrade PGRN. In addition, the stability of extracellular rhPGRN in the cell culture was checked by collecting conditioned medium from control cells after 72 hour of serum starvation, incubated with rhPGRN in the absence or in the presence of elastase. As shown in Fig. 2B right panel, PGRN seems to be remarkably stable in the neuronal medium. In contrast, extracellular PGRN was significantly degraded by exogenous elastase (Fig. 2B). Taken together, these results suggest that the pro-survival effect of added rhPGRN is most likely due to the full-length protein rather than to granulin peptides.

Serum withdrawal induces apoptosis

Cell death induced by serum deprivation showed characteristics of apoptosis. First of all, the examination of serum-deprived control and *GRN* KD cells after DAPI staining with a fluorescence microscopy revealed the abundance of chromatin condensation fragments (arrows) in the nuclei of *GRN* KD cells (Fig. 3A). On the other hand, fluorescent cell distribution using FLICA green fluorescent probe indicates higher activity of executive caspases 3 and 7 (Fig. 3B) in PGRN deficient cells when compared with control cells, as FLICA binds irreversibly to these enzymes when are activated [32], thus increasing the

fluorescence signal in apoptotic cells. Moreover, we observed that serum deprivation induced a higher release of cytochrome c to the cytosolic compartment in PGRN deficient cells than in control cells (Fig. 4). These results suggest the activation of the intrinsic (mitochondrial activated) pathway.

Role of CDK4/6/pRb pathway on cell survival

We had previously shown that PGRN deficit altered the activity of CDK4/6–associated kinase and survival of peripheral cells from FTLD-TDP patients bearing a *GRN* null mutation [29]. On these grounds, we were interested in evaluating the role of the CDK4/6/pRb pathway in the survival/death of control and PGRN-depleted neuroblastoma cell lines under serum deprivation conditions. Western blot analysis revealed a significant higher content of CDK4 and CDK6 in control cells, compared with KD cells. Consequently, an elevated CDK activity,as determined by the higher phosphorylation status of the retinoblastoma protein (pRb), was also observed in control cells (Fig. 5A). To investigate if CDK4/6 levels determine the ability of the *GRN* knockdown cells to survive in serum deprived medium, we inhibited CDK4/6 activity, either with an inhibitor of histone deacetylases (HDAC), such as sodium butyrate (SB), to blunt the *CDK4* and *CDK6* mRNA expression or with the small molecule PD332991 (Pfizer) that specifically inhibits the CDK4/6-associated kinase activity. Incubation of control cells with SB reduced CDK4 and CDK6 protein levels (Fig. 5A upper panel). Both SB and PD332991 inhibited CDK4/6-associated kinase activity as indicated by the decrease in the phosphorylation status of pRb (Fig. 5A, lower panel). In these conditions, control cells died as PGRN-depleted cells did (Fig. 5B).

Signaling pathways involved in the serum deprivation-mediated stimulation of cell death

Two signaling cascades have emerged as major players in the control of survival/death of many different cells: the mitogen-activated protein kinase (MAPK) and the phosphoinositide-3 kinase (PI3K) pathways [33-35]. Both pathways are more active in control than in *GRN* KD cells as indicated by the higher phosphorylation status of Akt and ERK1/2 (Fig. 6A). The potential participation of these signaling pathways in controlling cell survival was analyzed by using pharmacological inhibitors. We tested the effects of PD98059, inhibitor of MEK1/2, the upstream activator of ERK1/2, and LY294002, inhibitor of PI3K. We confirmed the effect of these inhibitors on the phosphorylation status of their respective kinases (Fig. 6B). LY294002 inhibited the Akt phosphorylation without affecting ERK1/2 phosphorylation status whereas PD98059 decreased ERK1/2 phosphorylation but did not modify Akt phosphorylation (Fig. 6A). As shown in Fig. 6B, both LY294002 and PD98059 sensitized control cells to cell death induced by

serum deprivation. Under these experimental conditions, control cells underwent apoptosis as did *GRN* KD cells. These findings suggest that PGRN deficiency impaired the activation of these two survival pathways. Inhibition of PI3K/Akt by LY294002, as well as the inhibition of ERK1/2 phosphorylation by PD98059 decreased the content of CDK6 in control cells to levels found in *GRN* KD cells (Fig. 7). Both inhibitors were also effective in decreasing the phosphorylation of pRb protein (Fig. 7). Taken together, these results suggest that cell fate (survival or death) ultimately relies on the activity of CDK6/pRb, which appear to be controlled by the PI3K/Akt and ERK1/2 pathways.

Exogenous PGRN normalizes the PI3K/Akt and ERK1/2 activity in *GRN* KD cells

We evaluated next whether the addition of rhPGRN to the incubation medium was able to increase PI3K/Akt and ERK1/2 activities. As shown in Fig. 8, rhPGRN restored the phosphorylation status of both Akt (Fig. 8A, left panel) and ERK1/2 (Fig. 8A, right panel) in PGRN deficient cells. In addition, it is shown that rhPGRN normalized CDK4 and CDK6 levels and pRb phosphorylation in *GRN* KD cells, reaching similar to control cells (Fig. 8B).

Effects of EGF and insulin on survival of *GRN* KD neuronal cells

Since PGRN deficiency seems to result in decreased PI3K/Akt and ERK1/2 activities, we sought to evaluate if *GRN* KD cells could be rescued from death induced by serum deprivation in the presence of other physiologically relevant activators of these pathways such as EGF or insulin [36,37]. As expected, both EGF and insulin increased the levels of pAkt and pERK1/2 (Fig. 9 upper panel). Under these conditions, *GRN* KD cells were able to survive in the absence of serum (Fig. 9 lower panel).

DISCUSSION

Loss-of-function *GRN* mutations are casually associated with FTLD, however, how the PGRN deficit induces specific neuronal death remains to be determined. In this work we have addressed the question as to whether knocking down the *GRN* gene in human neuroblastoma cells SH-SY5Y, determines the cell fate, survival/death, in response to a cell stressor like serum withdrawal. In addition, we have investigated the influence of PGRN deficiency on the PI3K/Akt and ERK1/2 signaling pathways. Our results indicate that PGRN deficient cells are more vulnerable to serum deprivation. The *GRN* KD cells show features of apoptosis, as increased activation of executive caspases and cytochrome c released from the mitochondria compared with control cells.

Addition of rhPGRN to the culture medium of *GRN* KD cells protects them from the serum withdrawal-induced apoptosis, suggesting that PGRN acts primarily through an extracellular mechanism. Interestingly, the effect of exogenous PGRN is most likely due to the full-length protein, rather than to granulin peptides.

In agreement with previous reports from this laboratory that revealed an important role for CDK4/6/pRb pathway in controlling survival of lymphoblasts from carriers of a loss-of-function *GRN* mutation [29], we observed in *GRN* KD neuroblastoma cells significant changes in the levels of CDK4 and CDK6 and the phosphorylation status of pRb protein. Increased signaling through CDK4/6/pRb pathway was associated with a survival advantage in both lymphoblasts and neuroblastoma cells. However, PGRN deficiency induced opposites changes in CDK4/6/pRb and cell resistance to serum deprivation in lymphoblasts and SH-SY5Y cells. Thus it seems that PGRN influences cell fate survival/death in cell type-specific manner. Exogenous rhPGRN was able to increase cell viability in *GRN* KD neuroblastoma cells to levels similar to control cells. In a similar way rhPGRN was able to restore the “normal” cell response to serum stimulation or withdrawal [29,38], by blunting the enhanced proliferative activity of PGRN-deficient lymphoblasts, or sensitizing cells to apoptosis in the absence or serum. The resistance of FTLD lymphoblasts towards a proapototic stimuli such as serum withdrawal may be explained by the tumor-like features of these cell lines, which it is believed reflects, at the systemic level, the proposed relationship between cellular stress and unscheduled cell cycle entry observed in susceptible neurons in neurodegenerative disorders [39,40]. Thus the possibility should be considered that the reduced CDK4/6/pRb activity, induced by PGRN deficiency in neuroblastoma cell lines could represent an attempt to blunt cell cycle progression of vulnerable neurons under conditions of chronic stress.

The involvement of CDK4/6/pRb in the control of the response of SH-SY5Y cells to serum deprivation is further supported by the fact that survival of control cells is reduced in the presence of specific inhibitors of either CDK4 and CDK6 expression levels or the CDK4/6-associated kinase activity such as SB or PD332991 respectively. The effects of these two drugs on survival of SH-SY5Y cells are in consonance with the reported effect of PD332991 on myeloma, increasing the cell sensitivity to bortezomib-induced apoptosis [41] and with the observation that knockdown of CDK6 enhanced the susceptibility of glioma cells to chemotherapy [42]. The fact that these drugs did not affect survival of PGRN-deficient cells, suggest a threshold for CDK4/6-associated kinase activity as the survival signal. Our results are in consonance with previous reports indicating a role of the CDK/pRb pathway in maintaining the postmitotic state throughout the lifetime of neurons [43]. Moreover, an anti-apoptotic role for CDK/pRb has been suggested, since a correlation between pRb loss and induction of apoptosis appears to occur in as pRb-/- null mice [44]. Nonetheless, our results contrast with other works suggesting a role of increased CDK6 activity in neuronal cell death [45,46], and neuroprotection through the inhibition of specific CDKs has been demonstrated [47,48]. Thus, it seems that activation of CDK/pRb can have a pro- or anti-apoptotic role in neuronal cells depending perhaps on the cell status or the nature of the cell stressor.

Analysis of the molecular signaling changes during serum deprivation in *GRN* knockdown cells revealed significant differences in the level of phosphorylated Akt and ERK1/2 compared with control cells. *GRN* KD cells showed impaired activation of both pathways. Treatment of control cells with the PI3K/Akt inhibitor LY294002 or the ERK1/2 inhibitor PD98059 induced significant apoptosis to levels similar to *GRN* KD cells. Therefore, it seems that PGRN may protect against apoptosis induced by serum withdrawal by activating the PI3K/Akt and ERK1/2 survival pathways. Indeed, we could observe the activating effects of rhPGRN in PI3K/Akt and ERK1/2 in PGRN-deficient neuroblastoma cells. This observation is in consonance with in previous reports showing the involvement of PGRN in activating these signaling pathways in a number of cell types [49,50], and in the reported anti-apoptotic effect of PGRN in primary neurons [51,22,52]. Moreover, activation of the PI3K/Akt and ERK1/2 pathways by EGF or insulin was sufficient to support survival of *GRN* KD cells in the absence of serum.

Our data suggest that CDK4/6 is a target of both PI3K/Akt and ER1/2 signaling pathways since the effects of LY294002 or PD98059 inducing apoptosis in control cells are accompanied by a significant decrease in CDK4 and CDK6 levels. In a similar way, ablation of Akt was shown to downregulate CDK4 and CDK6 expression [53,54]. Thus, it seems that PGRN-dependent PI3K/Akt and ERK1/2 activation

plays a critical role as mediator of cell survival by regulating the activity of the CDK4/6/pRb pathway. The proposed scenario is represented schematically in Fig. 10. The nature of the link between PGRN deficiency, PI3K/Akt and ERK1/2 signaling and CDK4/6/pRb activity remains to be resolved. Changes in signaling molecules and/or receptors can occur in PGRN deficiency, for example, alterations in circulating cytokines were detected in serum of FTLD patients carriers of a loss-of-function *GRN* mutation [55], and changes in Wnt signaling had been found in cells from FTLD patients [56,57]. This issue is currently under investigation in our laboratory.

Together, our data indicate a neuroprotective role for PGRN and provide further support for the premise that chronic PGRN deficiency in FTLD results in reduced survival signaling and increased neuronal vulnerability to cellular stressors, leading to increased rates of neuronal cell death. Treatment with exogenous PGRN or alternatively with activators of the PI3K/Akt and ERK1/2 pathways may be useful for prevention and treatment of FTLD-TDP associated to PGRN haploinsufficency.

Acknowledgements

This work has been supported by grants from Ministerio de Economía y Competitividad (SAF2011-28603) and Fundación Ramón Areces. AdlE is supported by Fundación Ramón Areces. We thank Drs. Joselin and Wu for providing the *GRN* KD SH-SY5Y cells.

Authors's contributions

Conceived and designed the experiments: AdlE and AMR. Performed the experiments: AdlE, CA, NE. Wrote the paper: AMR. Read and approved the final manuscript: AdlE, NE, CA, and AMR.

Conflict of interest statement

The authors declare that they have no conflict of interest.

REFERENCES:

1. Graff-Radford NR, Woodruff BK (2007) Frontotemporal dementia. Seminars in neurology 27 (1):48-57. doi:10.1055/s-2006-956755

2. Ratnavalli E, Brayne C, Dawson K, Hodges JR (2002) The prevalence of frontotemporal dementia. Neurology 58 (11):1615-1621

3. Boxer AL, Miller BL (2005) Clinical features of frontotemporal dementia. Alzheimer disease and associated disorders 19 Suppl 1:S3-6

4. Cairns NJ, Bigio EH, Mackenzie IR, Neumann M, Lee VM, Hatanpaa KJ, White CL, 3rd, Schneider JA, Grinberg LT, Halliday G, Duyckaerts C, Lowe JS, Holm IE, Tolnay M, Okamoto K, Yokoo H, Murayama S, Woulfe J, Munoz DG, Dickson DW, Ince PG, Trojanowski JQ, Mann DM (2007) Neuropathologic diagnostic and nosologic criteria for frontotemporal lobar degeneration: consensus of the Consortium for Frontotemporal Lobar Degeneration. Acta neuropathologica 114 (1):5-22. doi:10.1007/s00401-007-0237-2

5. Mackenzie IR, Neumann M, Cairns NJ, Munoz DG, Isaacs AM (2011) Novel types of frontotemporal lobar degeneration: beyond tau and TDP-43. Journal of molecular neuroscience : MN 45 (3):402-408. doi:10.1007/s12031-011-9551-1

6. Neumann M, Sampathu DM, Kwong LK, Truax AC, Micsenyi MC, Chou TT, Bruce J, Schuck T, Grossman M, Clark CM, McCluskey LF, Miller BL, Masliah E, Mackenzie IR, Feldman H, Feiden W, Kretzschmar HA, Trojanowski JQ, Lee VM (2006) Ubiquitinated TDP-43 in frontotemporal lobar degeneration and amyotrophic lateral sclerosis. Science (New York, NY) 314 (5796):130-133. doi:10.1126/science.1134108

7. Baker M, Mackenzie IR, Pickering-Brown SM, Gass J, Rademakers R, Lindholm C, Snowden J, Adamson J, Sadovnick AD, Rollinson S, Cannon A, Dwosh E, Neary D, Melquist S, Richardson A, Dickson D, Berger Z, Eriksen J, Robinson T, Zehr C, Dickey CA, Crook R, McGowan E, Mann D, Boeve B, Feldman H, Hutton M (2006) Mutations in progranulin cause tau-negative frontotemporal dementia linked to chromosome 17. Nature 442 (7105):916-919. doi:10.1038/nature05016

8. Cruts M, Gijselinck I, van der Zee J, Engelborghs S, Wils H, Pirici D, Rademakers R, Vandenberghe R, Dermaut B, Martin JJ, van Duijn C, Peeters K, Sciot R, Santens P, De Pooter T, Mattheijssens M, Van den Broeck M, Cuijt I, Vennekens K, De Deyn PP, Kumar-Singh S, Van Broeckhoven C (2006) Null

mutations in progranulin cause ubiquitin-positive frontotemporal dementia linked to chromosome 17q21. Nature 442 (7105):920-924. doi:10.1038/nature05017

9. Forman MS, Mackenzie IR, Cairns NJ, Swanson E, Boyer PJ, Drachman DA, Jhaveri BS, Karlawish JH, Pestronk A, Smith TW, Tu PH, Watts GD, Markesbery WR, Smith CD, Kimonis VE (2006) Novel ubiquitin neuropathology in frontotemporal dementia with valosin-containing protein gene mutations. Journal of neuropathology and experimental neurology 65 (6):571-581

10. Gitcho MA, Bigio EH, Mishra M, Johnson N, Weintraub S, Mesulam M, Rademakers R, Chakraverty S, Cruchaga C, Morris JC, Goate AM, Cairns NJ (2009) TARDBP 3'-UTR variant in autopsy-confirmed frontotemporal lobar degeneration with TDP-43 proteinopathy. Acta neuropathologica 118 (5):633-645. doi:10.1007/s00401-009-0571-7

11. Le Ber I, Camuzat A, Guerreiro R, Bouya-Ahmed K, Bras J, Nicolas G, Gabelle A, Didic M, De Septenville A, Millecamps S, Lenglet T, Latouche M, Kabashi E, Campion D, Hannequin D, Hardy J, Brice A (2013) SQSTM1 mutations in French patients with frontotemporal dementia or frontotemporal dementia with amyotrophic lateral sclerosis. JAMA neurology 70 (11):1403-1410. doi:10.1001/jamaneurol.2013.3849

12. Deng HX, Chen W, Hong ST, Boycott KM, Gorrie GH, Siddique N, Yang Y, Fecto F, Shi Y, Zhai H, Jiang H, Hirano M, Rampersaud E, Jansen GH, Donkervoort S, Bigio EH, Brooks BR, Ajroud K, Sufit RL, Haines JL, Mugnaini E, Pericak-Vance MA, Siddique T (2011) Mutations in UBQLN2 cause dominant X-linked juvenile and adult-onset ALS and ALS/dementia. Nature 477 (7363):211-215. doi:10.1038/nature10353

13. DeJesus-Hernandez M, Mackenzie IR, Boeve BF, Boxer AL, Baker M, Rutherford NJ, Nicholson AM, Finch NA, Flynn H, Adamson J, Kouri N, Wojtas A, Sengdy P, Hsiung GY, Karydas A, Seeley WW, Josephs KA, Coppola G, Geschwind DH, Wszolek ZK, Feldman H, Knopman DS, Petersen RC, Miller BL, Dickson DW, Boylan KB, Graff-Radford NR, Rademakers R (2011) Expanded GGGGCC hexanucleotide repeat in noncoding region of C9ORF72 causes chromosome 9p-linked FTD and ALS. Neuron 72 (2):245-256. doi:10.1016/j.neuron.2011.09.011

14. Murray ME, DeJesus-Hernandez M, Rutherford NJ, Baker M, Duara R, Graff-Radford NR, Wszolek ZK, Ferman TJ, Josephs KA, Boylan KB, Rademakers R, Dickson DW (2011) Clinical and neuropathologic heterogeneity of c9FTD/ALS associated with hexanucleotide repeat expansion in C9ORF72. Acta neuropathologica 122 (6):673-690. doi:10.1007/s00401-011-0907-y

15. Ahmed Z, Mackenzie IR, Hutton ML, Dickson DW (2007) Progranulin in frontotemporal lobar degeneration and neuroinflammation. Journal of neuroinflammation 4:7. doi:10.1186/1742-2094-4-7

16. Coppola G, Karydas A, Rademakers R, Wang Q, Baker M, Hutton M, Miller BL, Geschwind DH (2008) Gene expression study on peripheral blood identifies progranulin mutations. Annals of neurology 64 (1):92-96. doi:10.1002/ana.21397

17. Gijselinck I, Van Broeckhoven C, Cruts M (2008) Granulin mutations associated with frontotemporal lobar degeneration and related disorders: an update. Human mutation 29 (12):1373-1386. doi:10.1002/humu.20785

18. Bhandari V, Bateman A (1992) Structure and chromosomal location of the human granulin gene. Biochemical and biophysical research communications 188 (1):57-63

19. Daniel R, He Z, Carmichael KP, Halper J, Bateman A (2000) Cellular localization of gene expression for progranulin. The journal of histochemistry and cytochemistry : official journal of the Histochemistry Society 48 (7):999-1009

20. Petkau TL, Neal SJ, Orban PC, MacDonald JL, Hill AM, Lu G, Feldman HH, Mackenzie IR, Leavitt BR (2010) Progranulin expression in the developing and adult murine brain. The Journal of comparative neurology 518 (19):3931-3947. doi:10.1002/cne.22430

21. Eriksen JL, Mackenzie IR (2008) Progranulin: normal function and role in neurodegeneration. Journal of neurochemistry 104 (2):287-297. doi:10.1111/j.1471-4159.2007.04968.x

22. Van Damme P, Van Hoecke A, Lambrechts D, Vanacker P, Bogaert E, van Swieten J, Carmeliet P, Van Den Bosch L, Robberecht W (2008) Progranulin functions as a neurotrophic factor to regulate neurite outgrowth and enhance neuronal survival. The Journal of cell biology 181 (1):37-41. doi:10.1083/jcb.200712039

23. Hu F, Padukkavidana T, Vaegter CB, Brady OA, Zheng Y, Mackenzie IR, Feldman HH, Nykjaer A, Strittmatter SM (2010) Sortilin-mediated endocytosis determines levels of the frontotemporal dementia protein, progranulin. Neuron 68 (4):654-667. doi:10.1016/j.neuron.2010.09.034

24. Gao X, Joselin AP, Wang L, Kar A, Ray P, Bateman A, Goate AM, Wu JY (2010) Progranulin promotes neurite outgrowth and neuronal differentiation by regulating GSK-3beta. Protein & cell 1 (6):552-562. doi:10.1007/s13238-010-0067-1

25. Guo A, Tapia L, Bamji SX, Cynader MS, Jia W (2010) Progranulin deficiency leads to enhanced cell vulnerability and TDP-43 translocation in primary neuronal cultures. Brain research 1366:1-8. doi:10.1016/j.brainres.2010.09.099

26. Kleinberger G, Wils H, Ponsaerts P, Joris G, Timmermans JP, Van Broeckhoven C, Kumar-Singh S (2010) Increased caspase activation and decreased TDP-43 solubility in progranulin knockout cortical cultures. Journal of neurochemistry 115 (3):735-747. doi:10.1111/j.1471-4159.2010.06961.x

27. Ghoshal N, Dearborn JT, Wozniak DF, Cairns NJ (2012) Core features of frontotemporal dementia recapitulated in progranulin knockout mice. Neurobiology of disease 45 (1):395-408. doi:10.1016/j.nbd.2011.08.029

28. Yin F, Banerjee R, Thomas B, Zhou P, Qian L, Jia T, Ma X, Ma Y, Iadecola C, Beal MF, Nathan C, Ding A (2010) Exaggerated inflammation, impaired host defense, and neuropathology in progranulin-deficient mice. The Journal of experimental medicine 207 (1):117-128. doi:10.1084/jem.20091568

29. Alquezar C, Esteras N, Alzualde A, Moreno F, Ayuso MS, Lopez de Munain A, Martin-Requero A (2012) Inactivation of CDK/pRb pathway normalizes survival pattern of lymphoblasts expressing the FTLD-progranulin mutation c.709-1G>A. PloS one 7 (5):e37057. doi:10.1371/journal.pone.0037057

30. Mitsiades N, Mitsiades CS, Poulaki V, Chauhan D, Richardson PG, Hideshima T, Munshi N, Treon SP, Anderson KC (2002) Biologic sequelae of nuclear factor-kappaB blockade in multiple myeloma: therapeutic applications. Blood 99 (11):4079-4086

31. Samali A, Cai J, Zhivotovsky B, Jones DP, Orrenius S (1999) Presence of a pre-apoptotic complex of pro-caspase-3, Hsp60 and Hsp10 in the mitochondrial fraction of jurkat cells. The EMBO journal 18 (8):2040-2048. doi:10.1093/emboj/18.8.2040

32. Bedner E, Smolewski P, Amstad P, Darzynkiewicz Z (2000) Activation of caspases measured in situ by binding of fluorochrome-labeled inhibitors of caspases (FLICA): correlation with DNA fragmentation. Experimental cell research 259 (1):308-313. doi:10.1006/excr.2000.4955

33. Gerasimovskaya EV, Tucker DA, Weiser-Evans M, Wenzlau JM, Klemm DJ, Banks M, Stenmark KR (2005) Extracellular ATP-induced proliferation of adventitial fibroblasts requires phosphoinositide 3-kinase, Akt, mammalian target of rapamycin, and p70 S6 kinase signaling pathways. The Journal of biological chemistry 280 (3):1838-1848. doi:10.1074/jbc.M409466200

34. Katso R, Okkenhaug K, Ahmadi K, White S, Timms J, Waterfield MD (2001) Cellular function of phosphoinositide 3-kinases: implications for development, homeostasis, and cancer. Annual review of cell and developmental biology 17:615-675. doi:10.1146/annurev.cellbio.17.1.615

35. Meloche S, Pouyssegur J (2007) The ERK1/2 mitogen-activated protein kinase pathway as a master regulator of the G1- to S-phase transition. Oncogene 26 (22):3227-3239. doi:10.1038/sj.onc.1210414

36. Thomas CY, Chouinard M, Cox M, Parsons S, Stallings-Mann M, Garcia R, Jove R, Wharen R (2003) Spontaneous activation and signaling by overexpressed epidermal growth factor receptors in glioblastoma cells. International journal of cancer Journal international du cancer 104 (1):19–27. doi:10.1002/ijc.10880

37. Machado-Neto JA, Favaro P, Lazarini M, Costa FF, Olalla Saad ST, Traina F (2011) Knockdown of insulin receptor substrate 1 reduces proliferation and downregulates Akt/mTOR and MAPK pathways in K562 cells2. Biochimica et biophysica acta 1813(8):1404-1411. doi: 10.1016/j.bbamcr.2011.04.002

38. Alquezar C, Esteras N, Bartolome F, Merino JJ, Alzualde A, Lopez de Munain A, Martin-Requero A (2012) Alteration in cell cycle-related proteins in lymphoblasts from carriers of the c.709-1G>A PGRN mutation associated with FTLD-TDP dementia. Neurobiology of aging 33 (2):429 e427-420.

39. Zhu X, Raina AK, Perry G, Smith MA (2004) Alzheimer's disease: the two-hit hypothesis. The Lancet Neurology 3 (4):219-26. doi:10.1016/s1474-4422(4)00707-0

40. Zhu X, Lee HG, Perry G, Smith MA (2007) Alzheimer disease, the two-hit hypothesis: an update. Biochimica et biophysica acta 1772 (4):494-502. doi:10.1016/j.bbadis.2006.10.014

41. Menu E, Garcia J, Huang X, Di Liberto M, Toogood PL, Chen I, Vanderkerken K, Chen-Kiang S (2008) A novel therapeutic combination using PD 0332991 and bortezomib: study in the 5T33MM myeloma model. Cancer research 68 (14):5519-5523. doi:10.1158/0008-5472.can-07-6404

42. Li B, He H, Tao BB, Zhao ZY, Hu GH, Luo C, Chen JX, Ding XH, Sheng P, Dong Y, Zhang L, Lu YC (2012) Knockdown of CDK6 enhances glioma sensitivity to chemotherapy. Oncology reports 28 (3):909-914. doi:10.3892/or.2012.1884

43. Feddersen RM, Clark HB, Yunis WS, Orr HT (1995) In vivo viability of postmitotic Purkinje neurons requires pRb family member function. Molecular and cellular neurosciences 6 (2):153-167. doi:10.1006/mcne.1995.1014

44. White E (1994) Tumour biology. p53, guardian of Rb. Nature 371 (6492):21-22. doi:10.1038/371021a0

45. Greene LA, Liu DX, Troy CM, Biswas SC (2007) Cell cycle molecules define a pathway required for neuron death in development and disease. Biochimica et biophysica acta 1772 (4):392-401. doi:10.1016/j.bbadis.2006.12.003

46. Nguyen MD, Mushynski WE, Julien JP (2002) Cycling at the interface between neurodevelopment and neurodegeneration. Cell death and differentiation 9 (12):1294-1306. doi:10.1038/sj.cdd.4401108

47. Chen XC, Chen LM, Zhu YG, Fang F, Zhou YC, Zhao CH (2003) Involvement of CDK4, pRB, and E2F1 in ginsenoside Rg1 protecting rat cortical neurons from beta-amyloid-induced apoptosis. Acta pharmacologica Sinica 24 (12):1259-1264

48. Copani A, Caraci F, Hoozemans JJ, Calafiore M, Sortino MA, Nicoletti F (2007) The nature of the cell cycle in neurons: focus on a "non-canonical" pathway of DNA replication causally related to death. Biochimica et biophysica acta 1772 (4):409-412. doi:10.1016/j.bbadis.2006.10.016

49. Hu SY, Tai CC, Li YH, Wu JL (2012) Progranulin compensates for blocked IGF-1 signaling to promote myotube hypertrophy in C2C12 myoblasts via the PI3K/Akt/mTOR pathway. FEBS letters 586 (19):3485-3492. doi:10.1016/j.febslet.2012.07.077

50. Zanocco-Marani T, Bateman A, Romano G, Valentinis B, He ZH, Baserga R (1999) Biological activities and signaling pathways of the granulin/epithelin precursor. Cancer research 59 (20):5331-5340

51. Ryan CL, Baranowski DC, Chitramuthu BP, Malik S, Li Z, Cao M, Minotti S, Durham HD, Kay DG, Shaw CA, Bennett HP, Bateman A (2009) Progranulin is expressed within motor neurons and promotes neuronal cell survival. BMC neuroscience 10:130. doi:10.1186/1471-2202-10-130

52. Xu J, Xilouri M, Bruban J, Shioi J, Shao Z, Papazoglou I, Vekrellis K, Robakis NK (2011) Extracellular progranulin protects cortical neurons from toxic insults by activating survival signaling. Neurobiology of aging 32 (12):2326 e2325-2316. doi:10.1016/j.neurobiolaging.2011.06.017

53. Cariaga-Martinez AE, Lopez-Ruiz P, Nombela-Blanco MP, Motino O, Gonzalez-Corpas A, Rodriguez-Ubreva J, Lobo MV, Cortes MA, Colas B (2013) Distinct and specific roles of AKT1 and AKT2 in androgen-sensitive and androgen-independent prostate cancer cells. Cellular signalling 25 (7):1586-1597. doi:10.1016/j.cellsig.2013.03.019

54. Santi SA, Lee H (2011) Ablation of Akt2 induces autophagy through cell cycle arrest, the downregulation of p70S6K, and the deregulation of mitochondria in MDA-MB231 cells. PloS one 6 (1):e14614. doi:10.1371/journal.pone.0014614

55. Bossu P, Salani F, Alberici A, Archetti S, Bellelli G, Galimberti D, Scarpini E, Spalletta G, Caltagirone C, Padovani A, Borroni B (2011) Loss of function mutations in the progranulin gene are related to pro-inflammatory cytokine dysregulation in frontotemporal lobar degeneration patients. Journal of neuroinflammation 8:65. doi:10.1186/1742-2094-8-65

56. Alquezar C, Esteras N, de la Encarnacion A, Alzualde A, Moreno F, Lopez de Munain A, Martin-Requero A (2014) PGRN haploinsufficiency increased Wnt5a signaling in peripheral cells from frontotemporal lobar degeneration-progranulin mutation carriers. Neurobiology of aging 35 (4):886-898. doi:10.1016/j.neurobiolaging.2013.09.021

57. Rosen EY, Wexler EM, Versano R, Coppola G, Gao F, Winden KD, Oldham MC, Martens LH, Zhou P, Farese RV, Jr., Geschwind DH (2011) Functional genomic analyses identify pathways dysregulated by progranulin deficiency, implicating Wnt signaling. Neuron 71 (6):1030-1042. doi:10.1016/j.neuron.2011.07.021

FIGURE LEGENDS:

Fig. 1

Knockdown of *GRN* in SH-SY5Y neuroblastoma cells reduced cell viability following serum deprivation

Whole-cell extracts of SH-SY5Y clones expressing either the control vector or a target sequence of human *GRN* mRNA, were analyzed for the expression of *GRN* mRNA by quantitative RT-PCR (A), and protein levels by Western blotting using specific antibodies (B). β-actin levels were analyzed as loading controls. Values shown for the densitometric analyses are the mean ± standard error of the mean (SEM) for four experiments. **p<0.01 and ***p<0.001 significantly different from control cells. (C) Survival of control (open symbols) and *GRN* KD cells (filled symbols) following serum deprivation. A total of 60,000 cells per well were seeded in a 96-well plaque and incubated in the absence of serum for the time period indicated. Cell viability was determined by the MTT assay and expressed as percentage of the value at day 0. Data shown are the mean ± SEM for six determinations carried in triplicate. *p<0.05 and ***p<0.001 significantly different from control.

Fig. 2

Exogenous progranulin restores the survival of *GRN* KD cells

(A) A total of 600,000 control and *GRN* KD cells were seeded and incubated in serum-free DMEM medium during 72 hours in the absence or in the presence of 100 ng/ml of recombinant human progranulin (rhPGRN). Cell number was determined by counting the cells excluding trypan blue using a TC10™ Automated Cell Counter. Values shown are the mean ± SEM of seven experiments. ***p<0.001 significantly different from control cells; †††p<0.001 significantly different from untreated *GRN* KD cells. (B) rhPGRN (100 ng/ml) was incubated in the absence and presence of 0.1 U/ml of elastase for 3 hours (left panel) and the levels of PGRN protein were determined by Western blot. PGRN levels were also determined in conditioned medium from rhPGRN-treated cells in the absence or in the presence of elastase (right panel). Representative immunoblots are shown.

Fig. 3

Progranulin deficiency sensitizes cells to serum withdrawal-induced apoptosis

(A) Representative photomicrograph of 4,6-diamidino-2-phenylindole (DAPI)-stained control and *GRN* KD SH-SY5Y cells after 72 hours of serum deprivation. Arrows show the presence of chromatin condensation/fragmentation indicating apoptosis. (B) Caspase activation in serum-deprived control and *GRN* KD cells. Cells were incubated as above and then labeled with the FLICA reagent following the manufacture's recommendation to detect its binding to active caspases 3 and 7. A representative flow cytometric analysis of the frequency distribution of cells according to their green fluorescence is shown.

Fig. 4

Enhanced release of cytochrome c to the cytosol in serum-deprived *GRN* KD neuroblastoma SH-SY5Y cells

Control and *GRN* KD cells were serum deprived for 72 hours. Cell lysates were fractionated to isolate cytoplasmic and crude mitochondria. The presence of cytochrome c in cytosolic and mitochondrial fractions was assessed by Western blot analysis using the ApoTrack™ antibody cocktail, which demonstrates the purity of the fractions and loading. A representative blot is shown. Densitometric analyses are presented below. The data represent the mean ± SEM of the mitochondrial and cytosolic cytochrome c for four independent experiments. *$p<0.05$ and **$p<0.01$ significantly different from control cells.

Fig. 5

Effects of sodium butyrate and PD332991 on CDK4/6 protein levels, phosphorylation status of pRb and cell survival

(A) Control and *GRN* KD cells were incubated in serum-free medium for 72 hours in the absence or in the presence of 10 μM sodium butyrate (SB) or 1 μM PD332991. Representative immunoblots are shown. Densitometric analyses are presented in the right panel. Values shown are the mean ± SEM for ten experiments. ***$p<0.001$ significantly different from control cells and ††$p<0.01$; †††$p<0.001$ significantly different from untreated cells. (B) Cell survival was determined by the MTT assay and expressed as percentage of survival in untreated cells. Values shown are the mean ± SEM for four

independent experiments. **p<0.01 significantly different from control cells. †p<0.05 significantly different from untreated cells.

Fig. 6

Effects of PI3K/Akt and MEK1/2 kinase inhibitors on serum withdrawal-induced loss of cell viability

(A) Control and *GRN* KD cells were incubated in serum-free medium for 24 hours in the absence or in the presence of 10 μM LY294002 or 20 μM PD98059. The relative levels of activation of ERK1/2 and Akt were assessed by Western blot analysis using phospho-specific antibodies. Representative immunoblots are shown. Densitometric analyses are presented in the right panel. Values shown are the mean ± SEM of five experiments. *p<0.05 and ***p<0.001 significantly different from control cells and †††p<0.001 significantly different from untreated cells. (B) Control and *GRN* KD cells were incubated in the absence and in the presence of different kinases inhibitors as above. Cell viability was assessed by measuring the MTT reduction and expressed as percentage of cell survival in untreated control cells. Values shown are the mean ± SEM for seven experiments. ***p<0.001 significantly different from control cells and †††p<0.001 significantly different from untreated cells.

Fig. 7

Effects of PI3K/Akt and MEK1/2 kinase inhibitors on CDK4/6 levels and phosphorylation status of pRb in control and *GRN* KD neuroblastoma SH-SY5Y

Control and *GRN* KD cells were incubated in serum-free medium for 72 hours in the absence or in the presence of 10 μM LY294002 or 20 μM PD98059. The levels of CDK4, CDK6 and pRb were assessed by Western blot analysis using specific antibodies. Representative immunoblots are shown. Densitometric analyses are presented in the right panel. Values shown are the mean ± SEM of five to ten experiments. *p<0.05, ***p<0.001 significantly different from control cells. †p<0.05, ††p<0.01, †††p<0.001 significantly different from untreated control cells.

Fig. 8

Effects of rhPGRN on PI3K/Akt, ERK1/2, and CDK4/6/pRb pathways

(A) Control and *GRN* KD cells were incubated in serum-free medium for 24 hours in the absence or in the presence of 100 ng/ml of recombinant human progranulin (rhPGRN). Representative immunoblots for Akt and ERK1/2 are shown in the left, while densitometric analyses are presented in the right. Values shown are the mean ± SEM of five experiments. (B) Representative immunoblots showing the effects of rhPGRN in CDK4 and CDK6 levels and phosphorylation status of the pRb protein. Densitometric analyses of CDK4 and CDK6 levels are presented in the right panel. Values shown are the mean ± SEM of five experiments **$p<0.01$, ***$p<0.001$ significantly different from control cells. †$p<0.05$ significantly different from untreated *GRN* KD cells.

Fig. 9

Effects of EGF and insulin on survival of *GRN* KD neuroblastoma SH-SY5Y cells

Control and *GRN* KD cells were incubated in serum-free medium for 72 hours in the absence or in the presence of of 100 ng/ml of EGF or 100nM of insulin. Cell extracts for immunoblotting were prepared 24 hours after growth factor addition. Representative immunoblots showing the effects of EGF and insulin on pAkt and pERK1/2 levels are presented in the upper panel. Lower panel: Cell viability was assessed 72 hours after serum deprivation and addition of EGF or insulin, by measuring the MTT reduction. Values shown are the mean ± SEM for three experiments carried out in triplicate. * $p<0.05$ significantly different from control cells and † $p<0.05$, †† $p<0.01$ significantly different from untreated cells.

Fig. 10

Influence of PGRN deficiency on the activation of survival pathways under conditions of serum deprivation

Compared with control cells, *GRN* KD neuroblastoma SH-SY5Y cells showed reduced activation of both PI3K/Akt and ERK1/2 pathways in response to serum deprivation, which then results in decreased activity of CDK6/pRb and stimulation of apoptosis. Treatment of *GRN* KD cells with rhPGRN normalized the cell survival response. In contrast treatment of control cells with specific inhibitors of CDK4/6, PI3K/Akt and ERK1/2 pathways sensitized control cells to serum withdrawal-induced apoptosis.

Table 1

Summary of antibodies used for Western blotting

Antibody name	Company	Dilution
Anti-granulin (EPR3781)	Abcam (ab108608)	1:500
Cytochrome c Apoptosis WB Antibody Cocktail	Abcam (ab110415)	1:250
β-actin (ACTBD11B7)	Santa Cruz (sc-81178)	1:500
CDK4 (C-22)	Santa Cruz (sc-260)	1:500
CDK6 (C-21)	Santa Cruz (sc-177)	1:1000
Rb (C-15)	Santa Cruz (sc-50)	1:500
α-tubulin (B-5-1-2)	Santa Cruz (sc-23948)	1:1000
Phospho-Akt (Ser473) (D9E) XP	Cell Signaling (#4060)	1:1000
Akt1 (C-20)	Santa Cruz (sc-1618)	1:1000
Phospho-p44/42 MAPK (Erk1/2) (Thr202/Tyr204) XP	Cell Signaling (#4370)	1:2000
p44/42 MAP Kinase	Cell Signaling (#9102)	1:2000

Key: ERK, extracellular-regulated kinase; MAPK, mitogen-activated protein kinase.

Figure 1
Click here to download high resolution image

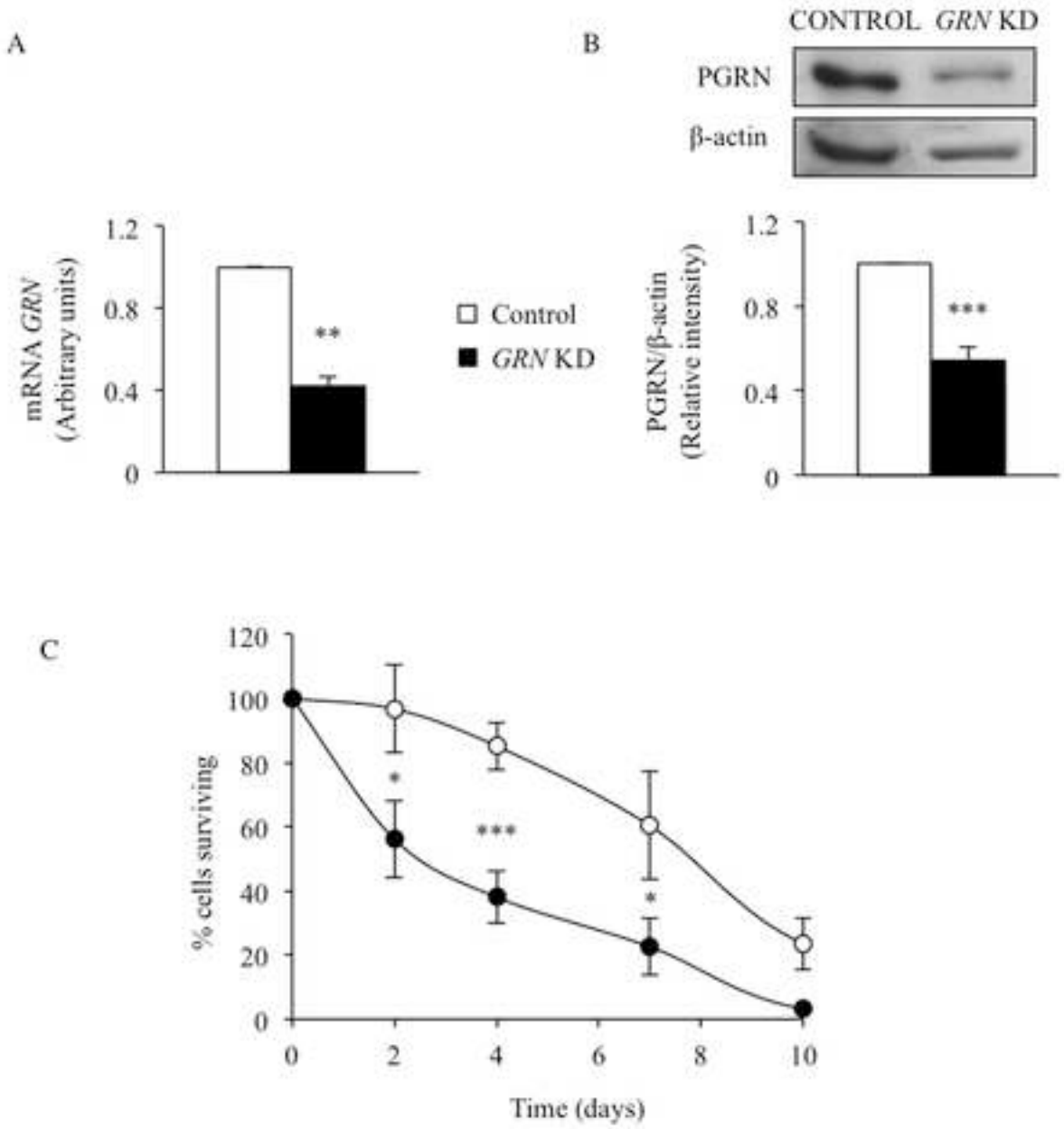

Fig. 1
de la Encarnación et al.

Figure 2
Click here to download high resolution image

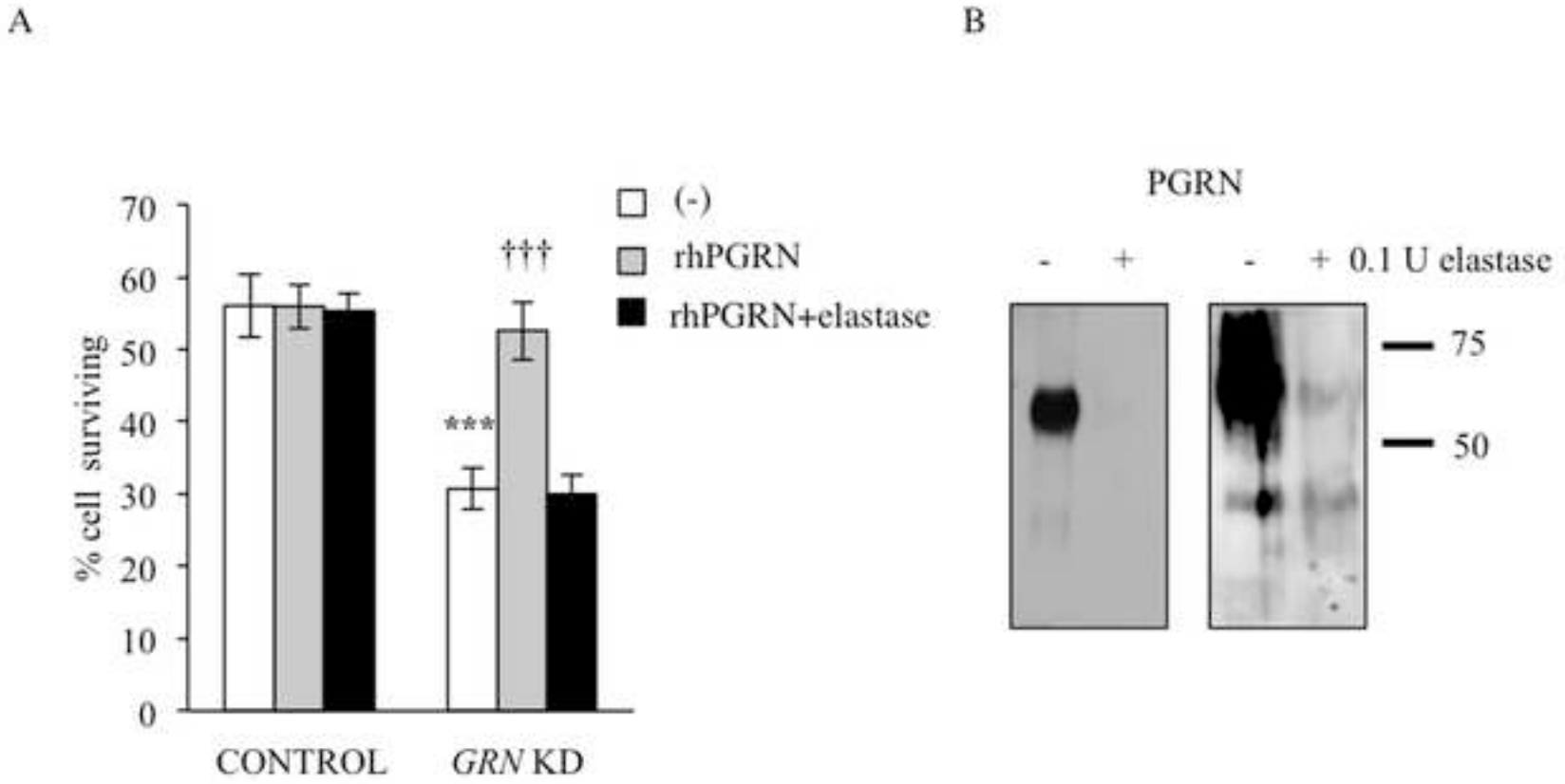

Fig. 2
de la Encarnación et al.

Figure 3
Click here to download high resolution image

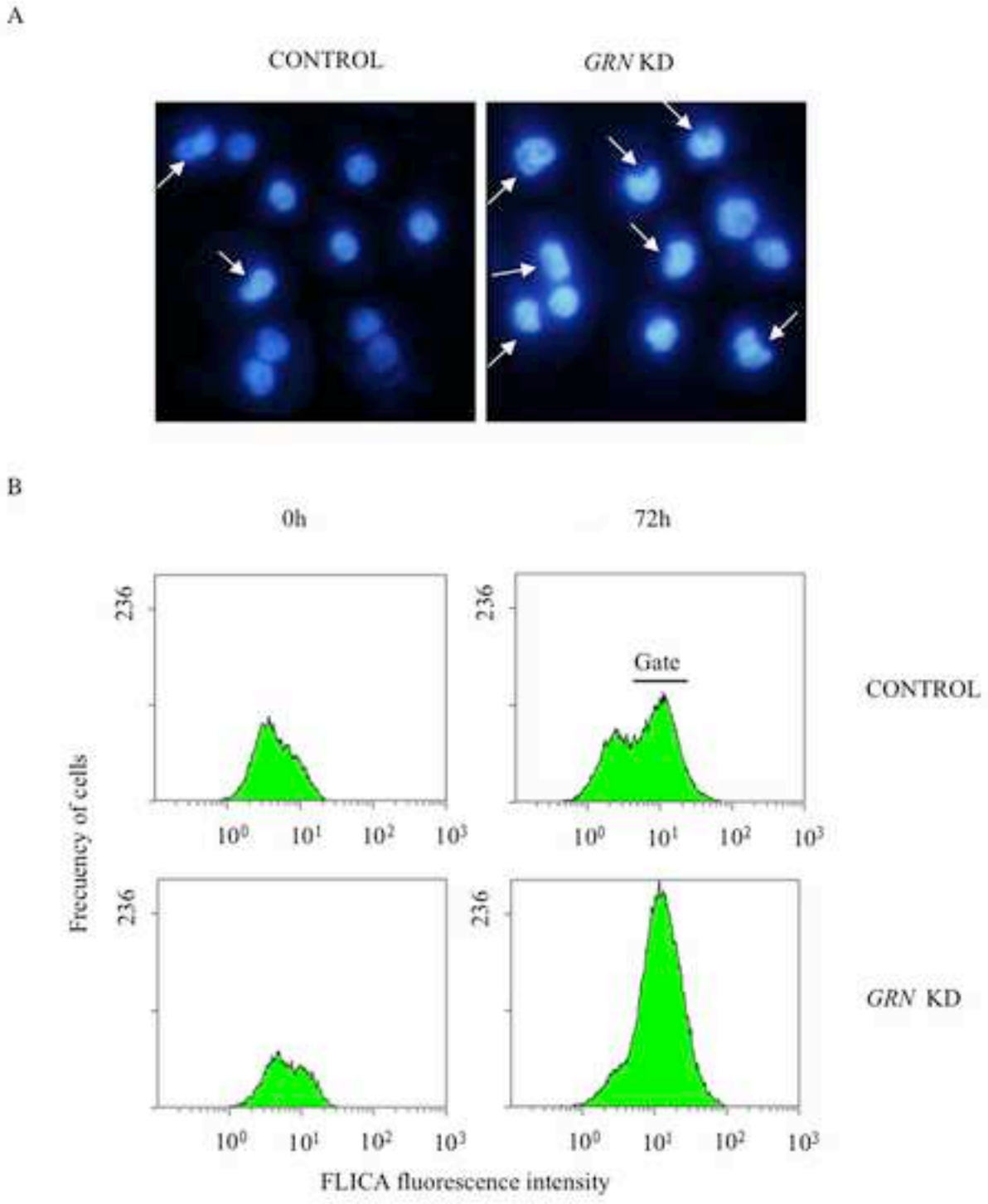

Fig. 3
de la Encarnación et al.

Figure 4
Click here to download high resolution image

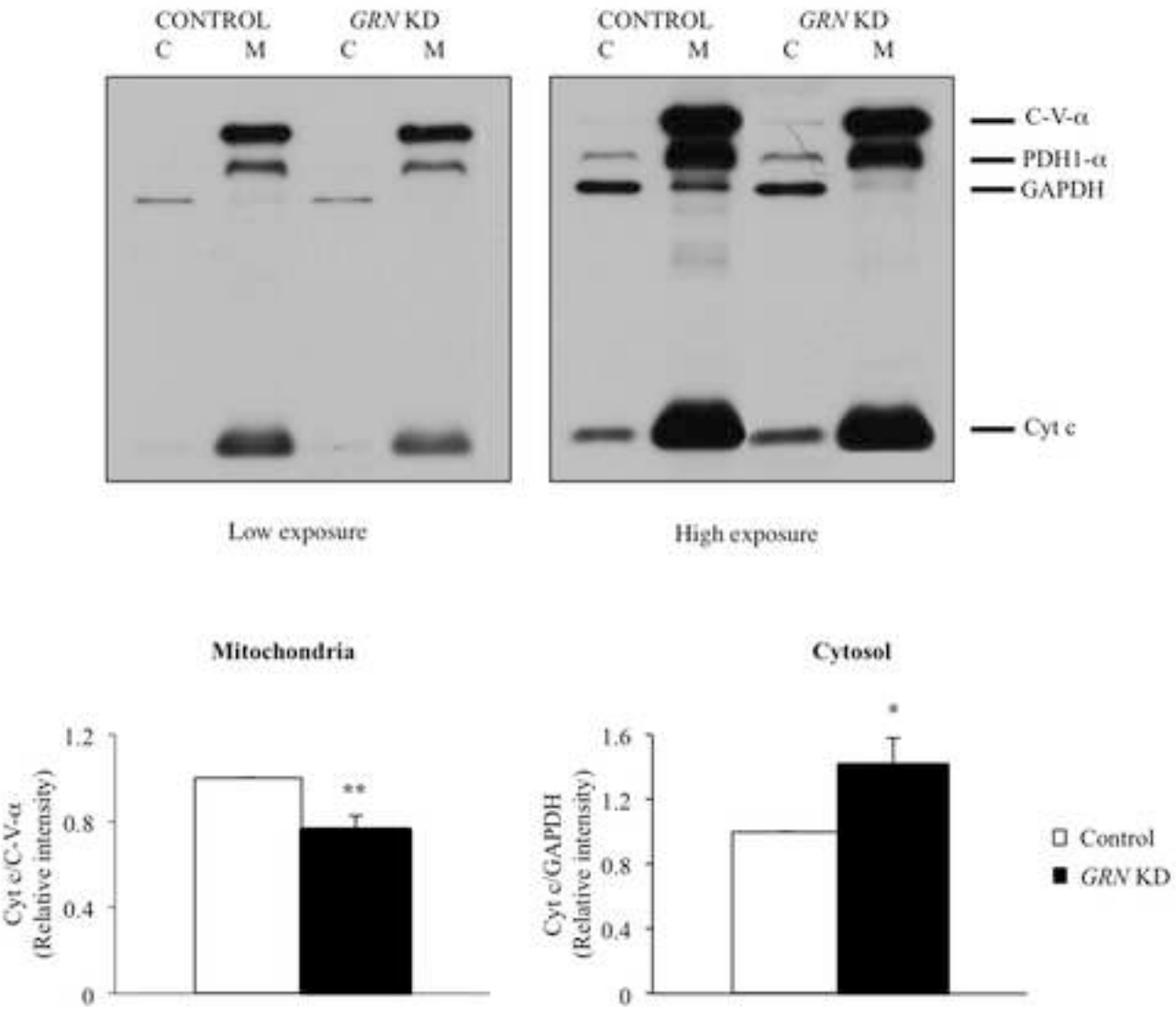

Fig. 4
de la Encarnación et al.

Figure 5
Click here to download high resolution image

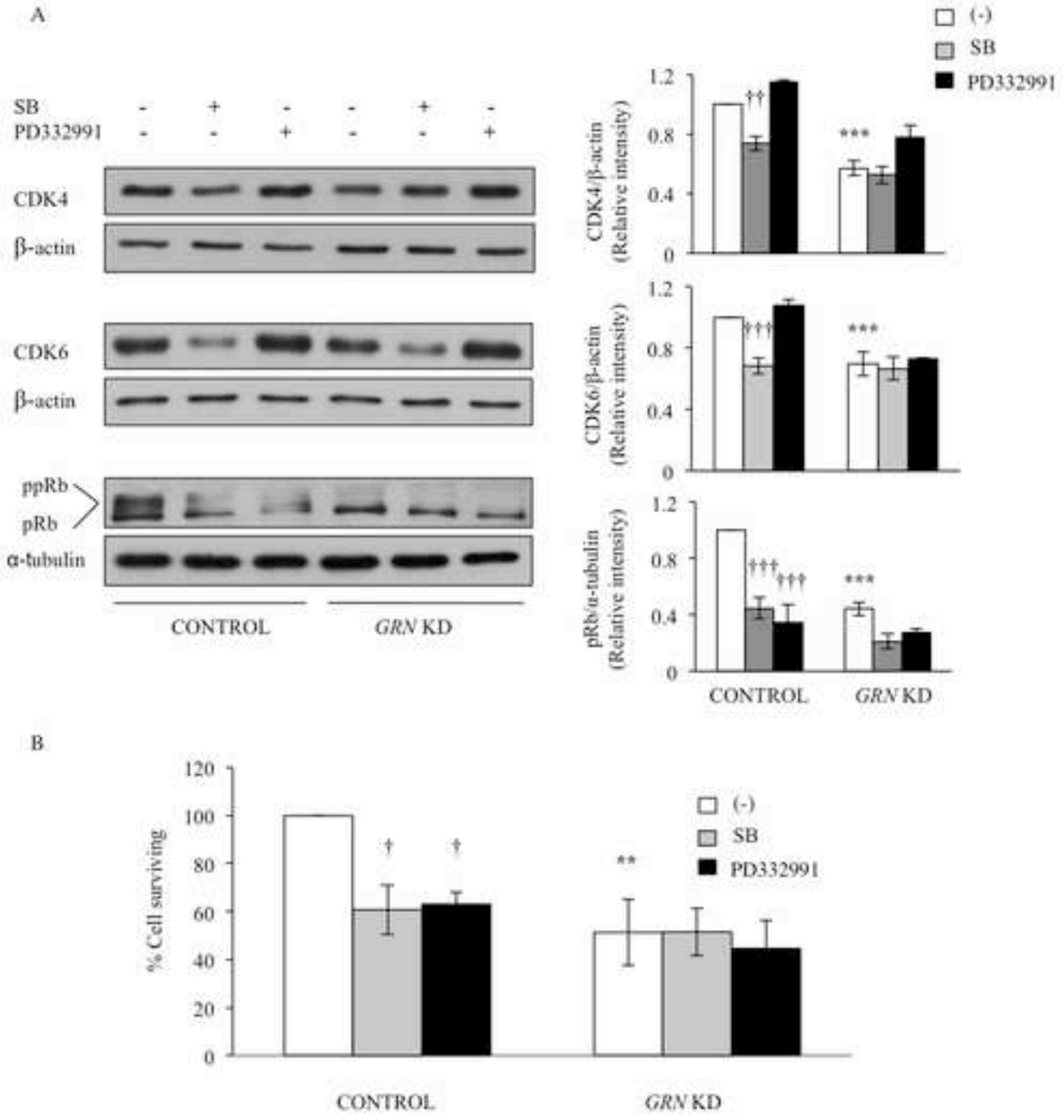

Fig. 5
de la Encarnación et al.

Figure 6
Click here to download high resolution image

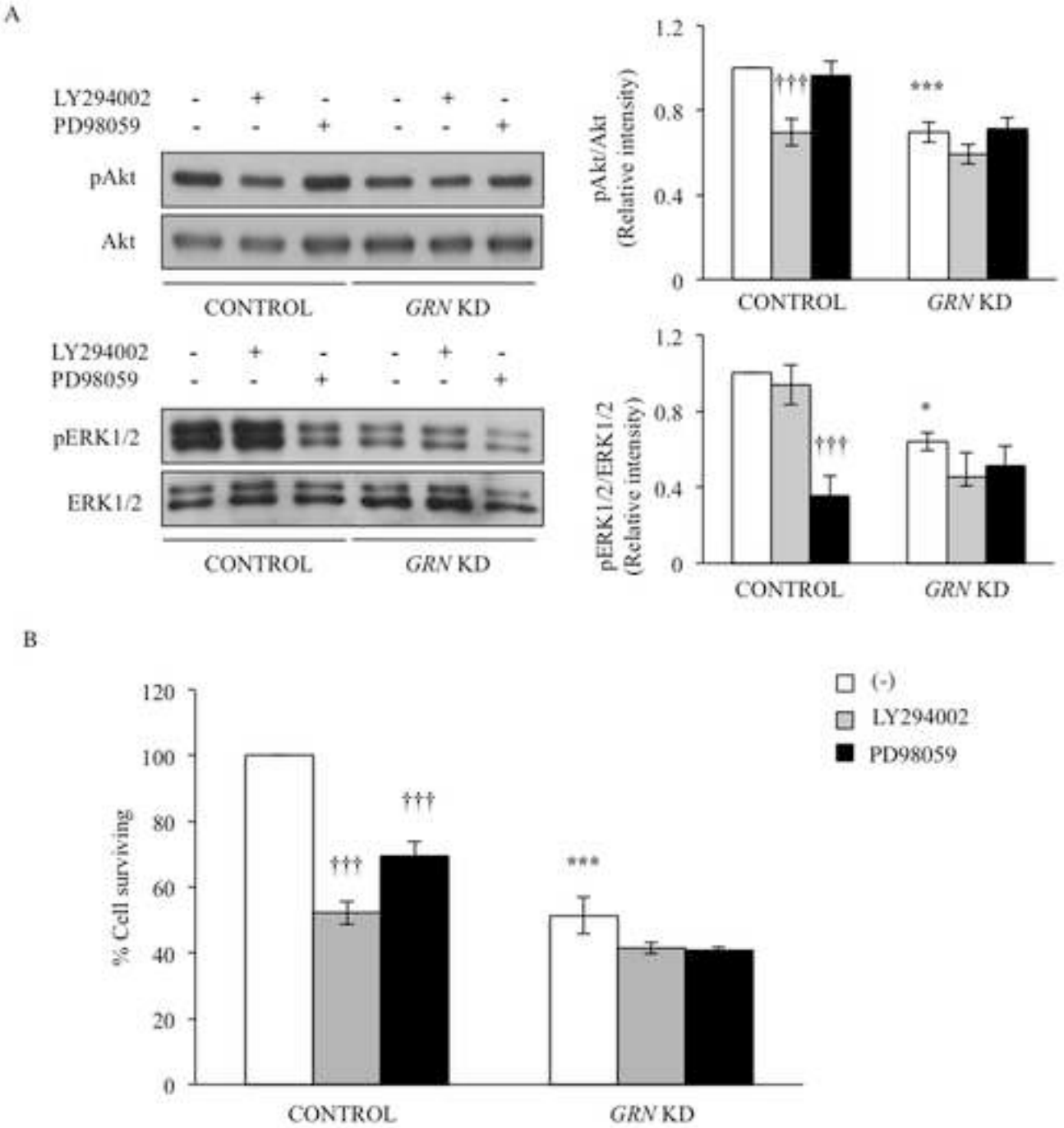

Fig.6
de la Encarnación et al.

Figure 7
Click here to download high resolution image

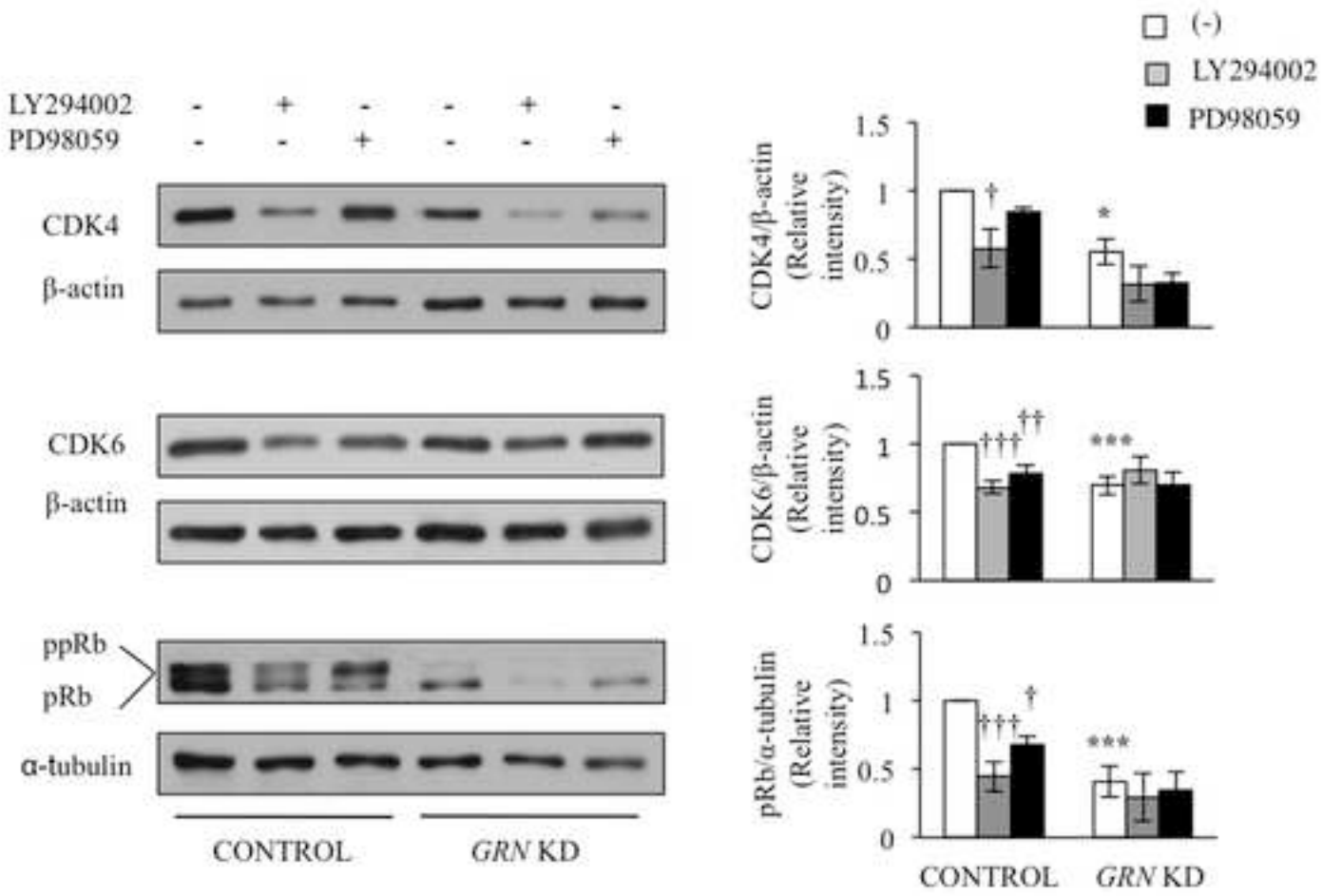

Fig.7
de la Encarnación et al.

Figure 8
Click here to download high resolution image

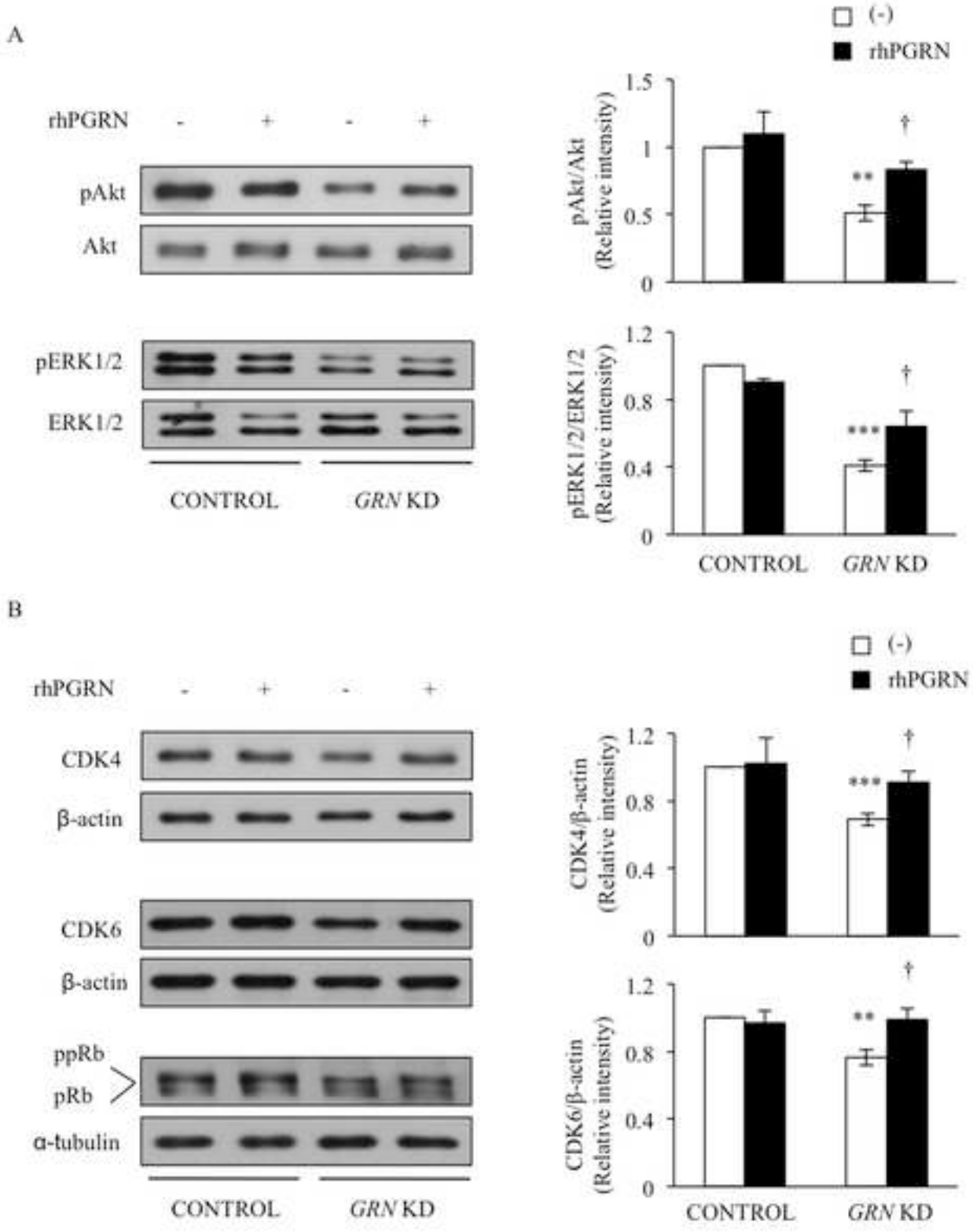

Fig. 8
de la Encarnación et al.

Figure 9
Click here to download high resolution image

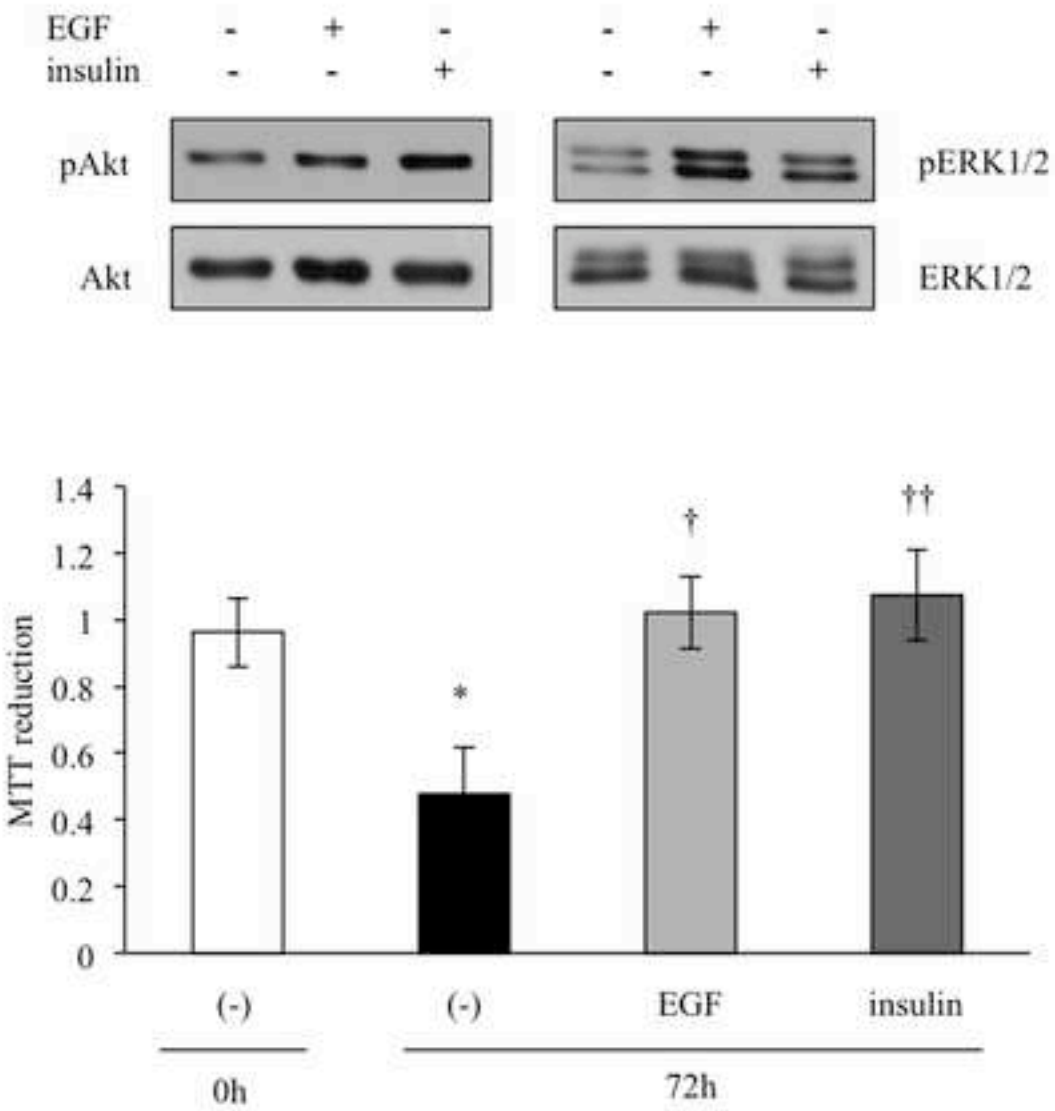

Fig. 9
de la Encarnación et al.

Figure 10
Click here to download high resolution image

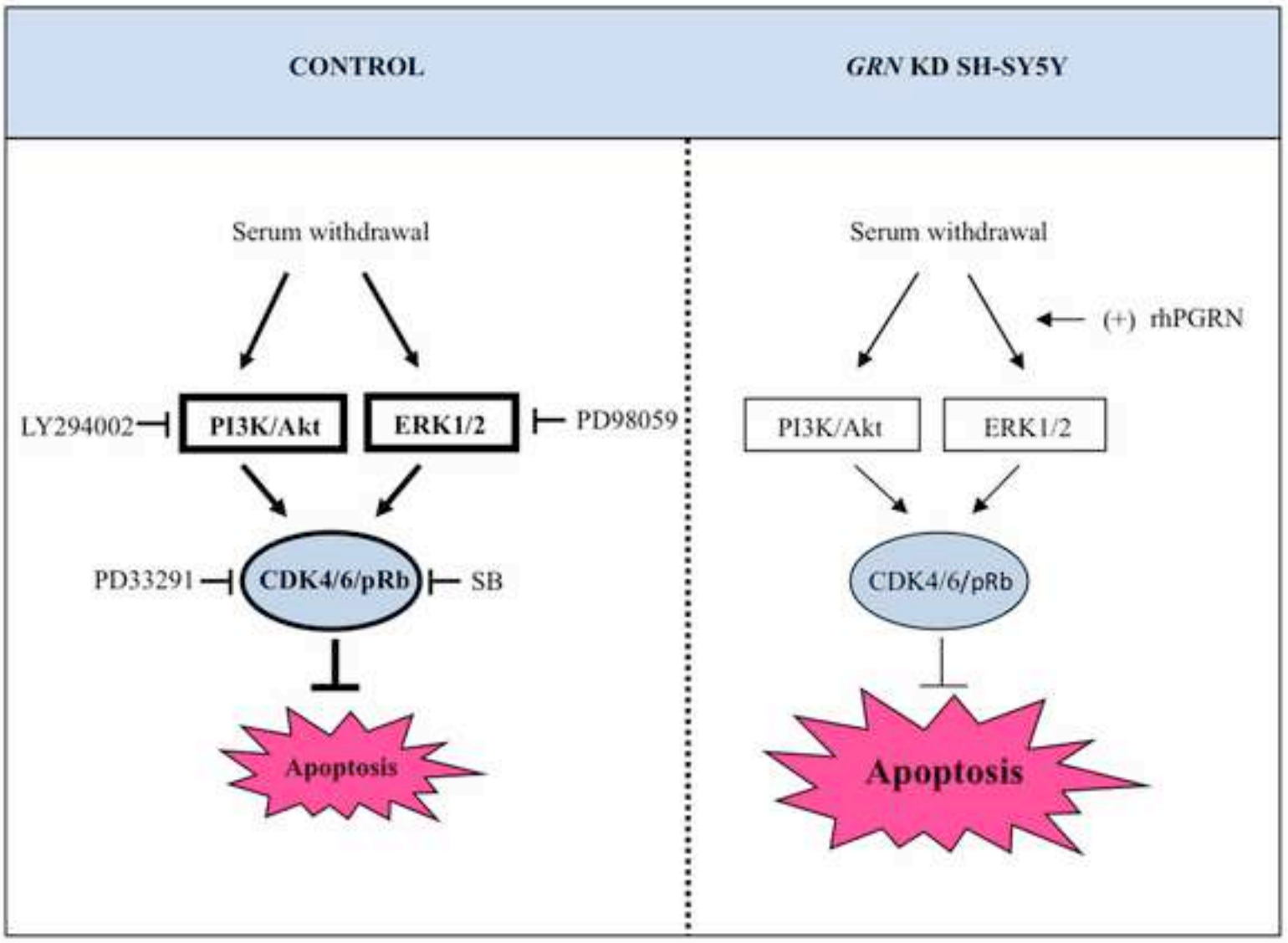

Fig. 10
de la Encarnación et al.